Yu. A. Teterin, *et al*.: Electronic Structure and Chemical Bond Nature in ...
Nuclear Technology & Radiation Protection: Year 2015, Vol. 30, No. 2, pp. 99-112

99

ELECTRONIC STRUCTURE AND CHEMICAL BOND NATURE IN $Cs_2PuO_2Cl_4$

by

Yury A. TETERIN [1,2*], *Konstantin I. MASLAKOV* [2], *Mikhail V. RYZHKOV* [3],
Anton Yu. TETERIN [1], *Kirill E. IVANOV* [1], *Stepan N. KALMYKOV* [2],
Vladimir G. PETROV [2], *and Dmitry N. SUGLOBOV* [4]

[1]NRC "Kurchatov Institute", Moscow, Russia
[2]Chemistry Department, Lomonosov Moscow State University, Moscow, Russia
[3]Institute of Solid State Chemistry, Ural Department of RAS, Ekaterinburg, Russia
[4]V.G. Khlopin Radium Institute, St.-Petersburg, Russia

X-ray photoelectron spectral analysis of dicaesiumtetrachlorodioxoplutonate ($Cs_2PuO_2Cl_4$) single crystal was done in the binding energy range 0- 35 eV on the basis of binding energies and structure of the core electronic shells (35 eV-1250 eV), as well as the relativistic discrete variation calculation results for the $PuO_2Cl_4^{2-}$ (D_{4h}). This cluster reflects Pu close environment in $Cs_2PuO_2Cl_4$ containing the plutonyl group PuO_2^{2+}. The many-body effects due to the presence of cesium and chlorine were shown to contribute to the outer valence (0- 15 eV binding energy) spectral structure much less than to the inner valence (15 eV- 35 eV binding energy) one. The filled Pu 5f electronic states were theoretically calculated and experimentally confirmed to present in the valence band of $Cs_2PuO_2Cl_4$. It corroborates the suggestion on the direct participation of the Pu 5f electrons in the chemical bond. The Pu 6p atomic orbitals were shown to participate in formation of both the inner and the outer valence molecular orbitals (bands), while the filled Pu 6p and O 2s, Cl 3s electronic shells were found to take the largest part in formation of the inner valence molecular orbitals. The composition of molecular orbitals and the sequence order in the binding energy range 0- 35 eV in $Cs_2PuO_2Cl_4$ were established. The quantitative scheme of molecular orbitals for $Cs_2PuO_2Cl_4$ in the binding energy range 0- 15 eV was built on the basis of the experimental and theoretical data. It is fundamental for both understanding the chemical bond nature in $Cs_2PuO_2Cl_4$ and the interpretation of other X-ray spectra of $Cs_2PuO_2Cl_4$. The contributions to the chemical binding for the $PuO_2Cl_4^{2-}$ cluster were evaluated to be: the contribution of the outer valence molecular orbitals –66 %, the contribution of the inner valence molecular orbitals –34 %.

Key words: X-ray photoelectron spectroscopy, valence molecular orbitals,
plutonyl group

INTRODUCTION

While doing the X-ray photoelectron spectroscopy (XPS) studies of actinide compounds containing the actinyl group AnO_2^{2+}, instead of a single doubly-degenerated atomic $An6p_{3/2}$ component, the XPS spectra manifested the two several eV distant from each other peaks [1-7]. Also in the 0-~35 eV binding energy (BE) range the observed peaks were several eV wide, which sometimes is wider than the corresponding core electron peaks [6, 7]. For example, the O 1s peak (E_b = 531.8 eV) full width at half maximum (FWHM) (Γ, eV) for $Cs_2PuO_2Cl_4$ is Γ = 1.8 eV, while the corresponding O 2s (E_b~25 eV) peak is ~4.0 eV wide and structured. This contradicts the Heisenberg

uncertainty ratio according to which the lower BE XPS atomic peaks are expected to be narrower. For $Cs_2AnO_2Cl_4$ (An = U, Np, Pu) [6-9] and UO_2X_2 (X = = Br, Cl, F) [5, 10] it is vice versa. It shows that the peaks observed in the 0-~35 eV BE range are not purely atomic. Formation of the inner (IVMO) and the outer (OVMO) valence molecular orbitals (MO) due to significant interaction of the An 6p and the O 2s filled atomic shells [6, 7, 11] could be the reason of this widening. Practically, these spectra observed as bands several eV wide reflect the valence band (0-~35 eV BE) structure.

From all actinide An(VI) compounds containing the almost linear actinyl group AnO_2^{2+}, uranyl compounds have been studied better in the low BE XPS range 0-~35 eV [1-7]. The XPS of uranyl compounds in the ~15 eV-~35 eV BE range (U6p and O2s AOs) in-

100

Yu. A. Teterin, *et al.*: Electronic Structure and Chemical Bond Nature in ...
Nuclear Technology & Radiation Protection: Year 2015, Vol. 30, No. 2, pp. 99-112

stead of the purely atomic single $U6p_{3/2,1/2}$ and $O2s$ peaks manifests the structure [1-5]. Taking into account the valence-core levels BE differences, FWHM and the structure interpretations, this structure in uranyl compounds was attributed to the effective (experimentally observed) OVMO and IVMO formation [3, 4, 6, 7].These data are in a qualitative and some quantitative agreement with the results of the non-relativistic [4, 12] and relativistic [13-16] calculations of the electronic structure of uranyl compounds. A special attention has been paid to the study of actinyl ions, whose electronic structure was considered in the non-relativistic approximation in [17, 18]. Position of Cs^+ ions regarding to the uranyl group containing clusters for some of the U(VI) compounds and the correlation of the U4f-O1s BE difference with the R_{U-O} interatomic distance, are given in [19]. The participation of the U6p and the O2s electrons in the U-O binding in uranyl group was considered in [20, 21]. Despite the fact that correlation of the OVMO- and IVMO-related structure parameters with physical and chemical properties of uranium compounds have been thoroughly studied, the role of the U 6p electrons in the chemical bond still is not clear. The valence XPS structure of neptunyl compounds was studied less than that of uranyl compounds [6-8]. The photoelectron and XPS studies paid great attention to plutonium dioxide PuO_2, where Pu is located in the center of a cube surrounded by oxygen ions (see references. in [22]). The dependence of the Pu4f BE [23]and the Pu5f intensity [24]on the number of the not bound Pu5f electrons was drawn. However, from plutonyl compounds (where Pu is in symmetrical surrounding) only $Cs_2PuO_2Cl_4$ valence XPS structure [9, 25] was studied.

Beside the OVMO and IVMO formation [6], the fine XPS structure can also result from the spin-orbit splitting (E_{sl}), multiplet splitting (E_{ms}), induced charge (E_{ind}), many-body perturbation (E_{sat}), dynamic effect (gigantic Coster-Kronig transitions), Auger process [7, 11]. Several mechanisms of the structure formation exhibited simultaneously with similar probability do not allow a correct interpretation of the XPS spectra. If one of the structure formation mechanisms prevails, parameters of such a structure correlate quantitatively with physical and chemical properties of the studied compound. Parameters of this structure bear information on: degree of delocalization and participation of electrons in chemical binding; electronic configuration and oxidation states of ions; density of uncoupled electrons on paramagnetic ions; degree of participation of filled electronic shells of metals and ligands in the OVMO and IVMO formation, structure and nature of the MO; local environment [6, 7, 11].

The 0-~35 eV BE XPS range is especially important since it reflects the MO structure and with the photoionization cross-sections in mind reflects the total valence density of occupied states. However, this BE range XPS interpretation requires understanding of how effective (experimentally observable)structure formation mechanisms manifest. Therefore, the core (~35 eV-1250 eV BE) XPS structure has to be studied in order to evaluate the contributions of certain structure formation mechanism to the valence band XPS [6, 7, 11].

The authors of [9, 25] considered qualitatively the XPS of $Cs_2PuO_2Cl_4$. The quantitative interpretation of the valence XPS structure of UO_2^{2+}-group containing compounds taking into account the photoelectron, conversion, emission and other X-ray spectral data as well as relativistic calculation results, was done for γ-UO_3 [16, 26, 27] and UO_2F_2 [10]. The present work quantitatively interpreted the XPS structure of $Cs_2PuO_2Cl_4$ single crystal in the BE range 0-~35 eV. The binding energies, core-valence BE differences, core electron spectral structure parameters (~35 eV to 1250 eV BE) were taken into account as well as the relativistic self-consisting field discrete variation (SCF RDV) calculation results for the $PuO_2Cl_4^{2-}$ (D_{4h}) cluster which reflects Pu close environment in $Cs_2PuO_2Cl_4$, in order to understand the chemical bond nature and to evaluate the contributions of the OVMO and the IVMO electrons to this bond.

EXPERIMENTAL

Samples

Crystalline double cesium and plutonyl chloride $Cs_2PuO_2Cl_4$ was prepared in the same way as $Cs_2UO_2Cl_4$ [28] by adding the stoichiometric quantity of cesium chloride to plutonyl acetate dissolved in a diluted hydrochloric acid and the following re-crystallization (see [29]). The ~7 mm 3 mm 1 mm $Cs_2PuO_2Cl_4$ sample for the XPS study was glued with conductive glue to a metallic substrate. During the XPS measurements, the sample surface was cleaned mechanically with a scraper. The CsCl sample was prepared as a tablet from finely dispersed powder pressed in in on Ti substrate.

X-ray photoelectron measurements

XPS spectra were measured with an electrostatic spectrometer HP 5059A using AlK$_{1,2}$ ($h\nu$ =1486.6 eV) radiation under 1.3 10^{-7} Pa at room temperature. The low-energy electrons gun was used for the compensation of sample charging during the photo-emission. The device resolution measured as the full width atthe half-maximum (FWHM) of the Au 4f$_{7/2}$ peak was 0.7 eV (see experimental in [3, 4, 33]).

The valence and the core electron XPS structure parameters for the studied sample confirm unambiguously the presence of $Cs_2PuO_2Cl_4$ on the substrate surface [9]. The studied samples were proven not to con-

tain more than 0.5 wt. % of impurities, since foreign peaks were not observed in the whole XPS BE range 0-1250 eV.

Quantitative elemental analysis of the studied samples layers several nanometer-deepwas done. It was based on the fact that the spectral intensity is proportional to the number of certain atoms in the studied sample. The following ratio was used: $n_i/n_j = (S_i/S_j)(k_j/k_i)$, where n_i/n_j is the relative concentration of the studied atoms, S_i/S_j is the relative core-shell spectral intensity, k_j/k_i is the relative experimental sensitivity coefficient. The following coefficients were used: 1.00 (C 1s); 2.80 (O 1s); 2.92 (Cl 2p); 2.48 (Cl 2s); 40.84 (Pu $4f_{7/2}$; see, *e. g.* [30, 31]). The stoichiometric composition was satisfactory for $Cs_2PuO_2Cl_4$.

CALCULATIONS

In $Cs_2PuO_2Cl_4$ plutonium is surrounded by two oxygen ions in the axial directions(plutonyl group PuO_2^{2+}) and by four chlorine ions in the equatorial plane. The crystal structure parameters are: $R_{Pu-O} = 0.1752(3)$ nm and $R_{Pu-Cl} = 0.26648(8)$ nm [29]. As it is expected, these parameters are lower than those for $Cs_2NpO_2Cl_4$: $R_{Np-O} = 0.1758(2)$ nm, $R_{Np-Cl} = 0.2657(5)$ nm [17] and $Cs_2UO_2Cl_4$: $R_{U-O} = 0.1774(4)$ nm, $R_{U-Cl} = 0.2671(1)$ nm [32]. The electronic structure calculations were done for the three clusters $PuO_2Cl_4^{2-}$ with interatomic distances: (a) $R_{Pu-O} = 0.171$ nm and $R_{Pu-Cl} = 0.262$ nm; (b) $R_{Pu-O} = 0.174$ nm and $R_{Pu-Cl} = 0.264$ nm; (c) $R_{Pu-O} = 0.176$ nm, and $R_{Pu-Cl} = 0.266$ nmin order to evaluate the influence of the interatomic distances on the MO energies in the Cl 3s BE range. To evaluate the orbital forces the calculations were done for: (a) $R_{Pu-O} = 0.1752$ nm and $R_{Pu-Cl} = 0.2665$ nm (equilibrium position, tab. 2); (b) $R_{Pu-O} = 0.1772$ nm and $R_{Pu-Cl} = 0.2665$ nm; (c) $R_{Pu-O} = 0.1752$ nm, and $R_{Pu-Cl} = 0.2685$ nm. In the case of the $PuO_2Cl_4^{2-}$ cluster the re-normalization of the valence oxygen and chlorine AO populations during the self-consistency was done.The latter model of small cluster boundary condition also allows one to include into the iterative scheme the stoichiometry of the compound and the possibility of charge redistribution between the outer atoms in the cluster and the surrounding crystal.In the present paper the electronic structure was calculated as in [33].

RESULTS AND DISCUSSION

Core-electron XPS structure of $Cs_2PuO_2Cl_4$

Electron BE in the 0-1250 eV range for $Cs_2PuO_2Cl_4$ are given in tab. 1. The data for PuO_2 [22], $Pu(NO_3)_4$ n $_2O$ [34], metallic Pu [35] and calculation results for atomic Pu [36], as well as photo-ionization cross-sections [37, 38] are given for comparison. The data for CsCl are given in square brackets (tab. 1) in the end of the column for PuO_2. The basic peaks of CsCl XPS in the BE range 0-1250 eV are intense and contain the structure related to many-body perturbation at the higher BE side. This structure makes it difficult to identify the XPS plutonium peaks. Therefore, the valence and core XPS structure of CsCl was studied carefully in the BE range 0-1250 eV. For example, the Cs3d XPS [E_b(Cs3$d_{5/2}$) = 724.5 eV] exhibits the 20 % and 50 % intensity regarding to the basic peaks satellites 11.8 eV and 23.6 eV, respectively, shifted from the basic peaks. The Cl2p XPS [E_b(Cl $2p_{3/2}$) = 198.6 eV] exhibits such satellites 8 % and 25 % intensity 10 eV and 19 eV shifted from the basic peaks, respectively. Since intensity of such satellite is known to drop as the BE decreases [11], the satellites in the valence XPS are expected to be of the least intensity. The Cs and Cl XPS structure, as well as the satellite structure complicates significantly the interpretation of $Cs_2PuO_2Cl_4$ XPS in the 0-1250 eV BE range.

The O 1s XPS of $Cs_2PuO_2Cl_4$ was observed as a widened single peak at E_b(O 1s) = 531.8 eV and FWHM Γ(O 1s) = 1.8 eV (fig. 1). The Pu 4f XPS from $Cs_2PuO_2Cl_4$, at the highest probability, shows the structure related to many-body perturbation attributable to an extra electronic transition within the filled and the vacant valence levels during the Pu 4f photo-emission (fig. 2). It appears as shake-up satellites, whose parameters reflect the MO structure. As a result, the Pu 4f XPS consists of the spin-orbit split doublet with E_{sl}(Pu 4f) = 12.6 eV, and the shake-up satellites at the higher BE side with E_{sat} = 3.4 eV. The satellite intensity ($I_{sat} = I_s/I_o$) calculated as the ratio of the XPS satellite area (I_s) to the basic peak area (I_o), was 20 %. Such structure parameters can determine the actinide ion oxidation state as An(VI) [7]. The Pu 4f XPS structure is typical for actinide oxidation state An(VI): U(VI) [10, 16], Np(VI) [8], and Pu(VI) [9]. The shake-up satellites are known to appear in the XPS of any core levels of plutonium compounds, and the satellite intensity decreases as the BE level decreases [22]. Unfortunately, such satellites are not well observed in the Pu4d XPS from $Cs_2PuO_2Cl_4$ expected to exhibit a spin-orbit split doublet E_{sl}(Pu 4d) = 48.0 eV (fig. 3). It is due to the relatively high Pu 4d FWHM Γ(Pu 4d) = 6.6 eV and the extra fine structure in all the Pu 4d XPS BE range. This structure can be attributed to the low intensity Cs $M_{4-5}N_{4-5}O_{2-3}$ Auger peaks. It does not allow an accurate determination of the Pu $4d_{3/2}$ BE, FWHM and the shake-up satellite position. Since the spin-orbit splitting E_{sl}(Pu 4d) = 48.0 eV for PuO_2 [22] and E_{sl}(Pu 4d)$_{Theor.}$ = 48.1 eV [42], the Pu $4d_{3/2}$ peak is expected at E_b(Pu $4d_{3/2}$) = 851.5 eV (fig. 3 and tab. 1). The Pu $4p_{3/2}$ peak was observed at E_b(Pu $4p_{3/2}$) = 1128.9 eV. The Pu $4p_{3/2}$ BE range XPS exhibits the complex structure that does not allow a correct determination of the FWHM and the shake-up parameters [7, 9].

102

Yu. A. Teterin, *et al.*: Electronic Structure and Chemical Bond Nature in ...
Nuclear Technology & Radiation Protection: Year 2015, Vol. 30, No. 2, pp. 99-112

Table 1. Electron binding energies E_b [eV] and photo-ionization cross-sections σ [a] at 1486.6 eV

Pu nlj O nlj	$Cs_2PuO_2Cl_4$	PuO_2[b]	$Pu(NO_3)_4$ nH_2O[c]	Pu[d]	Pu_{Theor}[e]	σ
Pu5f	2.9 (2.1)[f]	2.6 (2.5)	4.1	~0.6	0.6	25.5
Pu6p$_{3/2}$	16.1	17.9 (2.8)	19.5	17.2	18.6	5.20
	21.0(3.1)					
Pu6p$_{1/2}$	32.0(3.0)	30.1(2.5)	31.4	29.2	30.5	1.76
		33.9		32.0		
Pu6s	51.7 (7.0)	50.1(4.0)		45.2	51.7	
				52.7		2.33
Pu5d$_{5/2}$	107.6(2.9)	104.6	106.0	101.3	103.1	51.2
Pu5d$_{3/2}$	~117.7(4.3)	~110.9	118.3	113.7	118.9	34.8
Pu5p$_{3/2}$	215	210.5	217.4	211.1	220.5	32.5
	218	215.5				
Pu5p$_{1/2}$				284.2	285.4	9.23
		278.7(2.9)				
Pu5s	~359			353.1	355.6	10.4
				365.1		
Pu4f$_{7/2}$	428.7(1.9)	426.1(2.0)	427.1	422.1	422.4	424
Pu4f$_{5/2}$	441.3(1.9)	438.8(1.9)	439.8	435.1	436.2	333
Pu4d$_{5/2}$	803.5(6.6)	801.4(6.0)	803.9	798.1	802.2	243
Pu4d$_{3/2}$	851.5	849.4 (6.0)	851.9	844.8	850.3	158
Pu4p$_{3/2}$	1128.9	1125.1(6.8)		1122.6	1127.7	109
O2p	~6.0	~4.9				0.27
O2s	25.3(3.1)	22.4	25.8			1.91
	27.9(2.5)		27.2			
O1s	531.8(1.8)	530.1(1.1)	533.0			40.0
Cs6s						0.16
Cs5p$_{3/2}$	10.4 (1.2)	[10.1(1.2)][f]				4.52
Cs5p$_{1/2}$						2.31
Cs5s	23.7(1.3)	[23.4(1.4)]				2.50
Cl3p		[4.4(1.4)]				2.35
Cl3s	16.1(1.8)	[15.0(1.2)]				2.52
Cl2p$_{3/2}$	198.6 (1.2)	[198.6(1.2)]				20.6
N1s			407.6			24.5

[a] Photo-ionozation cross-sections σ (kilobarn per atom, *i. e.*, 10^{-25} m^2 per atom) from [43]; [b] Values for PuO_2 from [22]; [c] Values for $Pu(NO_3)_4$ nH_2O from [40]; [d] Values for metallic Pu from [41]; [e] calculation data from [42], values given relative to the Pu5f peak from metallic Pu; [f] FWHM are given in parentheses, the values on CsCl are given in brackets

The dynamic effect related to the gigantic Coster-Kronig transitions, appears in *e. g.*, the Pu 5p XPS of $Cs_2PuO_2Cl_4$ superimposed with the Cl 2p electron energy loss spectrum (EELS) [7].

The multiplet splitting was expected to appear with the higher probability in the An 5d XPS [7, 11, 22]. Indeed, the Pu 5d spectrum instead of a spin-orbit split doublet (E_{sl}(Pu5d)$_{Theor.}$ = 15.8 eV [36]) exhibits a complicated structure with the Pu 5d$_{5/2}$ maximum at 107.6 eV (fig. 4). Similar structure was observed in the Pu 5d XPS from PuO_2 and oxides of other actinides [22, 39]. This structure can be explained by the multiplet splitting superimposed with the shake-up satellites. Therefore, it is difficult to separate the satellite-related structure and to determine the satellite intensities. Going from PuO_2 to $Cs_2PuO_2Cl_4$ the Pu 5d XPS structure changes significantly. The distance between the most explicit peaks grows from 6.3 eV to 10.1 eV (tab. 1), and the structure becomes similar to

that of the U 5d in UO_2 [7, 39]. It can be explained by the fact that the initial state electronic configuration of uranium in UO_2 and that of plutonium in $Cs_2PuO_2Cl_4$ is An$_5$f$_2$, which results in the similar XPS structure related to multiplet splitting. At the lower BE side from the Pu 5d$_{5/2}$ XPS peak, the Cs 4d satellite was observed. The multiplet splitting is very likely to show up in the Ln 4s XPS from lanthanide oxides [11]. In the Ln 5s XPS, the probability is about twice as low. Therefore, the Pu 5s and the Pu 6s XPS are expected to exhibit the multiplet splitting [7].

Despite this, one can separate the two peaks in the Pu 5p$_{3/2}$ component at 215 eV and at 218 eV BE (tab. 1). The similar splitting was observed in the Pu 5p$_{3/2}$ XPS from PuO_2 [22, 39]. With the data on the Ba 4p [40] and the Ln 4p [11, 41, 42] XPS in mind, one can attribute the Pu 5p structure to the dynamic effect. It results in the Pu ion complex final state consisting of the ground one-hole state Pu5p^{5}5d^{10}5f^n and the ex-

Table 2. MO compositions (parts) and energies E_0 [a] [eV] for the $PuO_2Cl_4^{-2}$ cluster (RDV) and photoionization cross-sections σ_i [b]

MO		$-E_0$ [eV]	MO composition											O		Cl	
			Pu														
			6s	6p1/2	6p3/2	6d3/2	6d5/2	7s	5f5/2	5f7/2	7p1/2	7p3/2	2s	2p	3s	3p
		σ_i 1.15		0.87	1.29	0.63	0.57	0.11	4.26	3.96	0.05	0.06	0.96	0.07	1.26	0.47
OVMO	$28\gamma_6^+$	−14.45				0.29	0.50	0.09					0.06	0.05		0.01
	$31\gamma_6^-$	−8.78							0.01	0.93	0.02		0.01	0.01		0.02
	$22\gamma_7^+$	−8.72				0.05	0.78							0.04	0.02	0.11
	$21\gamma_7^+$	−8.36				0.33	0.49							0.10	0.01	0.07
	$30\gamma_6^-$	−8.25							0.02	0.96				0.01		0.01
	$27\gamma_6^+$	−8.22				0.47	0.33	0.01						0.15		0.04
	$24\gamma_7^-$	−8.12		0.01								0.97			0.01	0.01
	$26\gamma_6^+$	−7.30				0.05	0.02	0.82						0.01	0.02	0.08
	$20\gamma_7^+$	−5.57				0.44	0.41									0.15
	$29\gamma_6^-$	−5.32		0.01	0.07				0.11	0.35	0.01		0.02	0.42		0.01
	$23\gamma_7^-$	−2.37							0.07	0.65				0.24		0.04
	$28\gamma_6^-$	−1.31							0.37	0.31				0.23		0.09
	$27\gamma_6^-$	−1.28							0.06	0.78				0.03		0.13
	$22\gamma_7^-$	−1.03							0.05	0.81						0.14
	$21\gamma_7^-$	−0.34							0.62	0.07						0.31
	$20\gamma_7^{-(c)}$	0.00							0.73	0.15				0.02		0.10
	$25\gamma_6^+$	0.80														1.00
	$26\gamma_6^-$	1.03			0.02				0.02	0.01		0.01		0.05		0.89
	$19\gamma_7^+$	1.05					0.01							0.06		0.93
	$24\gamma_6^+$	1.06				0.01								0.06		0.93
	$19\gamma_7^-$	1.30			0.01				0.05	0.03		0.01		0.02		0.88
	$25\gamma_6^-$	1.38							0.11	0.01						0.88
	$18\gamma_7^-$	1.39			0.01				0.05	0.07				0.01		0.86
	$17\gamma_7^-$	1.57			0.01				0.33	0.01				0.01		0.64
	$24\gamma_6^-$	1.73			0.01				0.04	0.06	0.01			0.02	0.01	0.85
	$18\gamma_7^+$	1.91				0.06	0.08									0.86
	$17\gamma_7^+$	2.25				0.05	0.07								0.03	0.85
	$23\gamma_6^+$	2.44				0.01	0.01	0.04						0.06	0.02	0.86
	$23\gamma_6^-$	3.18		0.01	0.07				0.11	0.33		0.01	0.01	0.36		0.10
	$22\gamma_6^+$	4.10	0.01				0.03	0.02					0.06	0.85	0.01	0.02
	$16\gamma_7^-$	4.15			0.02				0.11	0.18				0.67		0.02
	$16\gamma_7^+$	4.35				0.04	0.13							0.80		0.03
	$21\gamma_6^+$	4.45				0.13	0.05							0.79		0.03
	$22\gamma_6^-$	4.45		0.01					0.26	0.04				0.69		
IVMO	$21\gamma_6^-$	11.97			0.32				0.01	0.01		0.01	0.43	0.09	0.13	
	$15\gamma_7^-$	12.77			0.09							0.01			0.89	
	$15\gamma_7^+$	13.36				0.02	0.03								0.95	
	$20\gamma_6^-$	13.37		0.01	0.03				0.01	0.01			0.09		0.84	0.01
	$20\gamma_6^+$	13.47				0.01	0.01	0.02							0.95	0.01
	$14\gamma_7^-$	17.19			0.86									0.02	0.10	0.02
	$19\gamma_6^+$	18.84	0.02			0.04	0.05						0.86	0.03		
	$19\gamma_6^-$	21.89		0.16	0.45				0.01	0.01			0.32	0.04	0.01	
	$18\gamma_6^-$	28.71		0.79	0.03								0.12	0.05		0.01
	$18\gamma_6^+$	46.80	0.97										0.02	0.01		

[a] Levels shifted by 7.23 eV toward the positive values (upward); [b] Photo-ionization cross-sections σ_i (kilobarn per atom, *i. e.*, 10^{-25} m² per atom), for O and Cl from [37] and Pu from [38]; [c] HOMO (highest occupied MO) (two electrons), occupation number for all the orbitals is 2

cited two-hole $Pu5p^65d^85f^{n+1}$ state. This suggestion is based on the Pu 5p and the Pu 5d binding energy ratio $E_b(Pu\ 5p_{3/2})$ 218 eV and $E_b(Pu\ 5d_{5/2}) = 107.6$ eV, which satisfies the condition: $E_b(Pu\ 5p_{3/2})$ $2\ E_b(Pu\ 5d_{5/2})$. As a result, the probability of an extra excited two-hole final $Pu5p^65d^85f^{n+1}$ state after the Pu 5p photo-emission grows.

The Pu 5s XPS of $Cs_2PuO_2Cl_4$ is expected around $E_b(Pu\ 5s) \sim359$ eV [7]. The Pu 5s XPS from metallic plutonium is observed in about 35 eV wide range and consists of the two structured ~10 eV wide peaks at 353.1 eV and 365.1 eV [35]. This structure can be attributed to both the multiplet splitting and the dynamic effect. The Pu 6s XPS shows a widened (Γ(Pu

104

Yu. A. Teterin, *et al.*: Electronic Structure and Chemical Bond Nature in ...
Nuclear Technology & Radiation Protection: Year 2015, Vol. 30, No. 2, pp. 99-112
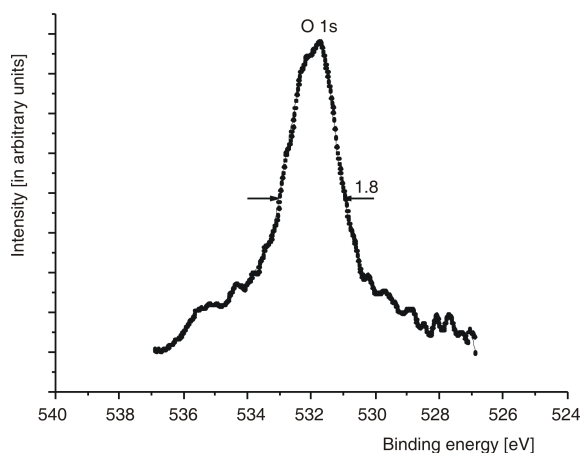
Figure 1. O 1s XPS from Cs$_2$PuO$_2$Cl$_4$
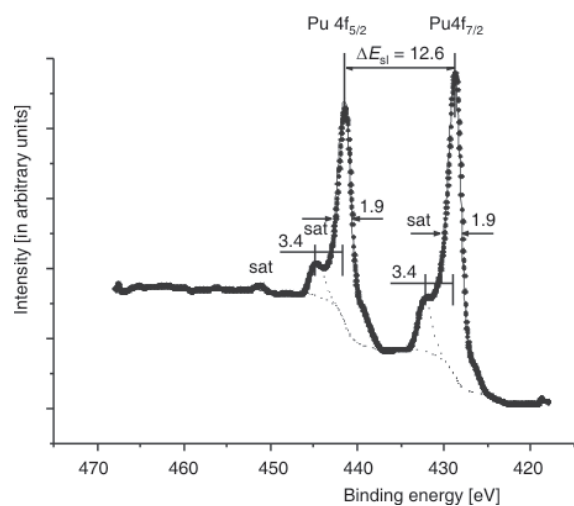
Figure 2. Pu 4f XPS from Cs$_2$PuO$_2$Cl$_4$
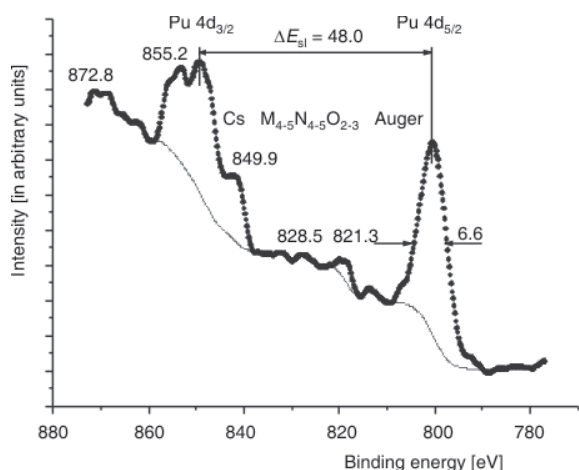
Figure 3. Pu 4d XPS from Cs$_2$PuO$_2$Cl$_4$

6s) = 7.0 eV) structured line at 51.7 eV BE [7]. One of the reasons for this Pu 6s XPS structure can be suggested the dynamic effect with the interaction of the
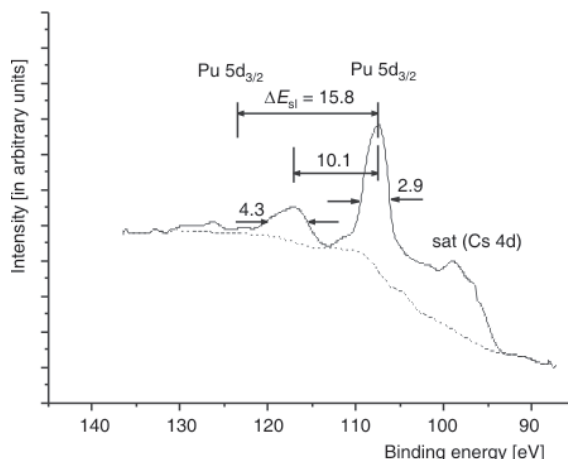
Figure 4. Pu 5d XPS from Cs$_2$PuO$_2$Cl$_4$

configurations of the final states like Pu $6s^1 6p^6 5f^n$ and Pu $6s^2 6p^4 5f^{n+1}$. Indeed, for the E_b(Pu 6s) = 51.7 eV, E_b(Pu $6p_{3/2}$) = 16.2 eV and E_b(Pu $6p_{1/2}$) = 30.4, the condition E_b(Pu 6s) ~ 2 E_b(Pu 6p) is satisfied, which does not contradict the possibility of the suggested configurations. The multiplet splitting- and the shake-up satellite- related structures are also possible in these spectra. It complicates the conclusion on the Pu 6s electrons participation in the MO formation based on the Pu 6s XPS parameters.

Since the An 6p BE range XPS going from Cs$_2$UO$_2$Cl$_4$ to Cs$_2$NpO$_2$Cl$_4$ and Cs$_2$PuO$_2$Cl$_4$, does not differ significantly, and the number *n* of the quasi-atomic An $5f^n$ electrons in the row U^{6+}($5f^0$), Np^{6+}($5f^1$), and Pu^{6+}($5f^2$) grows from 0 to 2 [7-9], one can suggest that the multiplet splitting does not contribute much to the valence (~15 eV-~35 eV BE) XPS structure. The extra structure related to the dynamic effect in this BE range has also low probability, because of the atomic electronic states but the quasi-atomic Pu 5f ones are absent in the valence BE range. As a result, the valence XPS structure can be associated with the MO formation, except for the spin-orbit split doublet at E_b(Cs $5p_{3/2}$) = 10.4 eV with E_{sl}(Cs 5p) = 1.6 eV, and the Cs 5s peak at E_b(Cs 5s) = = 23.7 eV (fig. 5). As it was noted, the extra structure in this BE range can also take place due to the EELS appeared at the higher BE side from the Cs 5p and Cs 5s XPS peaks. Therefore, fig. 5 bunder the low BE Cs$_2$PuO$_2$Cl$_4$ XPS gives the corresponding CsCl XPS normalized by the Cs 5p intensity in order to show the Cs 5p, 5s contribution to the Cs$_2$PuO$_2$Cl$_4$ XPS.

Electronic structure of the PuO$_2$Cl$_4^{2-}$ cluster

Electronic configuration of plutonium ground state $^7F_0$ can be presented as [Rn] $6s^2 6p^6 5f^6 6d^0 7s^2 7p^0$, where [Rn] is radon electronic configuration, and the other electronic shells are valence and can participate in the MO formation with the O $2s^2 2p^6$ and Cl $3s^2 3p^5$ AO in the
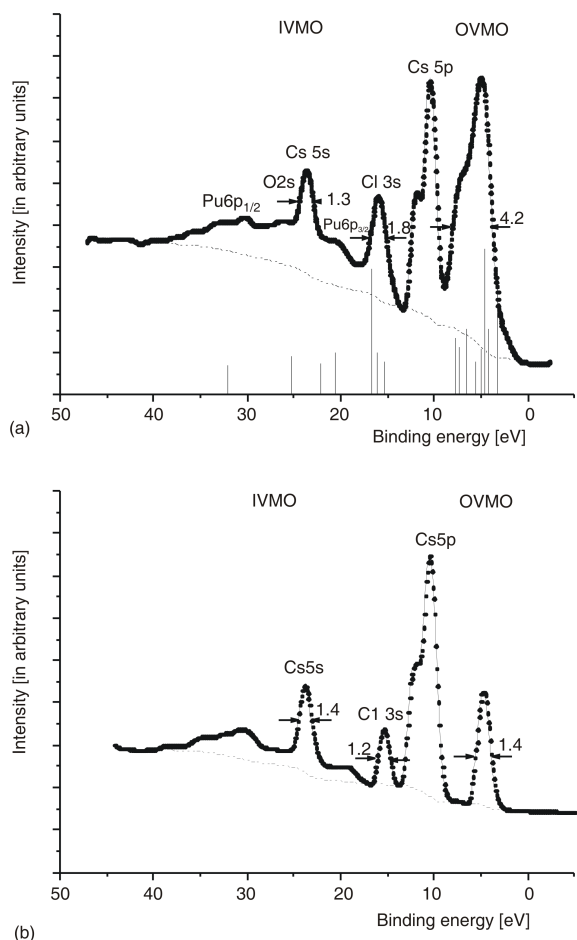
Figure 5. Valence band XPS; (a) – XPS from Cs₂PuO₂Cl₄ with the secondarily scattered electrons background. The vertical bars show the calculated (RDV) spectrum; (b) – XPS from CsCl with the subtracted secondarily scattered electrons background. Spectra normalized by the Cs 5p intensity

$PuO_2Cl_4^{2-}$ cluster. Results of the RDV electronic structure calculation of the $PuO_2Cl_4^{2-}$(D$_{4h}$) cluster reflecting Pu close environment structure in Cs₂PuO₂Cl₄ are given in tab. 2. This calculation technique employed the MO LCAO (molecular orbitals as linear combinations of atomic orbitals) method, which allowed a discussion about the chemical bond nature in terms of atomic and molecular orbitals. Indeed, the chemical bond formation and the AO overlapping result in the OVMO and the IVMO formation. Beside the Pu 6s,6p,5f,6d,7s, O 2s, 2p, and Cl 3s, 3p AO, these MO include the Pu 7p states, which are absent in atomic plutonium. The RDV calculations show that the Pu 6s AO, as well as the Pu 7s and Pu 7p AO, participate insignificantly in the MO formation (tab. 2). While the Pu 5f AO participate mostly in the OVMO formation, the Pu 6p, 6d AO participate in formation of both the OVMO and the IVMO. The largest Pu $6p_{3/2}$ and the O 2s AO mixing of the neighboring plutonium and oxygen was observed for the $21\gamma^{6-}$ (4) and the $19\gamma_6^-$ (9) IVMO (tab. 2). The Pu_$6p_{1/2}$-O 2s AO mixing in the $19\gamma_6^-$ (9) and the $18\gamma_6^-$ (10) IVMO are much higher than that in PuO₂ [22] because the interatomic distance

R_{Pu-O} in the plutonyl group is lower than that in PuO₂. A significant mixing was observed only for the Pu $6p_{3/2}$ and the Cl 3s AO with formation of the $15\gamma_7^-$ (5) and the $14\gamma_7^-$ (7) IVMO. The obtained results suggest subdividing the valence MO into the three groups. The first group: $20\gamma_7^-$-$22\gamma_6^-$ OVMO. The second group: $21\gamma_6^-$(4), $19\gamma_6^+$ (8), $19\gamma_6^-$(9), $18\gamma_6^-$(10), and $18\gamma_6^+$ IVMO characterizing the Pu-O binding in the axial direction. The third group: from $15\gamma_7^-$(5), $15\gamma_7^+$, $20\gamma_6^-$, $20\gamma_6^+$(6) to $14\gamma_7^-$(7) IVMO characterizing the Pu-Cl binding in the equatorial plane (tab. 2). These results allow one to understand the fine valence XPS structure of Cs₂PuO₂Cl₄.

The experimental valence band XPS of Cs₂PuO₂Cl₄ exhibits a complicated structure (fig. 5). It can be suggested to consist of the XPS of the $PuO_2Cl_4^{2-}$ ion and two cesium Cs⁺ ions. The valence XPS of the $PuO_2Cl_4^{2-}$ cluster is superimposed with the Cs5s²5p⁶6s⁰ XPS of the two Cs⁺ ions. Therefore, the CsCl XPS is given under the Cs₂PuO₂Cl₄ XPS, fig. 5(b). For comparison the XPS spectra were normalized by the Cs 5p intensity. The low BE CsCl XPS contains extra peaks at the higher BE side from the basic Cs 5s and Cs 5p peaks attributed to the shake-up satellites and other energy loss spectra. These extra peaks complicate the interpretation of the Cs₂PuO₂Cl₄ XPS. The contribution of this extra structure was taken into account based on the analysis of the Cs₂PuO₂Cl₄ and CsCl satellite structure in the 0-1250 eV BE range. It has to be taken into account that the XPS from Cs⁺ ion in Cs₂PuO₂Cl₄ can change compared to that from Cs⁺ in CsCl. To evaluate this contribution the difference spectrum was drawn. It was obtained by subtraction of the Cs⁺ XPS consisting of the Cs5s, 5p peaks with satellites from the Cs₂PuO₂Cl₄ XPS without taking into account the back scattering-related background (fig. 6). Despite the approximation inaccuracy, the resulting spectrum agrees qualitatively with the calculated spectrum for the $PuO_2Cl_4^{2-}$ cluster reflecting plutonium close environment in Cs₂PuO₂Cl₄.

To draw the difference spectrum, the XPS Cs₂PuO₂Cl₄ and CsCl intensities were normalized to the Cs5p spin-orbit doublet [E_{sl}(Cs5p) = 1.6 eV] intensity. It has to be noted that goingon from CsCl to Cs₂PuO₂Cl₄ the Cs 5s and the Cs 5p peaks shift to the higher BE region by 0.3 eV, and the Cl 3s peak – shifts by 1.1 eV (tab. 1).The difference spectrum was drawn for two cases: (a) without secondary scattered electrons-related background subtraction from the initial spectra; (b) with secondary scattered electrons- related background subtraction from the initial spectra (fig. 6). Despite the complicated structure, the difference spectra are in a good qualitative agreement.

The difference XPS characterizes the electronic structure of the $PuO_2Cl_4^{2-}$ cluster and reflects its valence electrons structure (fig. 6). In the 0-~35 eV BE range it can be conditionally subdivided into the two ranges. The first range 0-~15 eV exhibits the OVMO-related structure. These OVMO are formed

106

Yu. A. Teterin, *et al*.: Electronic Structure and Chemical Bond Nature in ...
Nuclear Technology & Radiation Protection: Year 2015, Vol. 30, No. 2, pp. 99-112
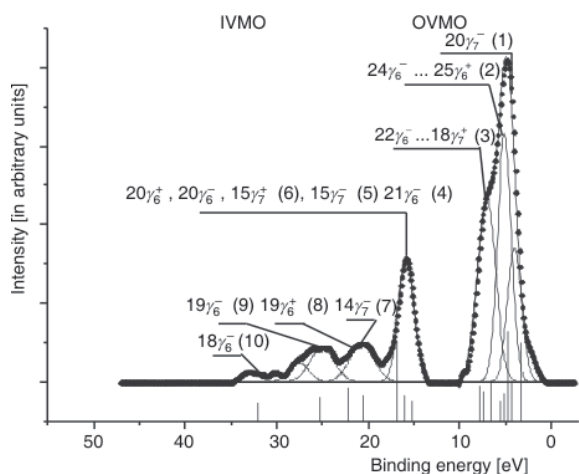
Figure 6. The difference of the valence XPS of Cs$_2$PuO$_2$Cl$_4$ and 2 Cs$^+$ ions with the subtracted secondarily scattered electrons background (see fig. 5)

mostly from the Pu 5f, 6d, 7s, 7p, the O 2p and the Cl 3p AO of the neighboring atoms. The second range ~15 eV-~35 eV exhibits the IVMO-related structure. These IVMO appear mostly due to the strong interaction of the completely filled Pu 6p and O 2s,Cl3s AO.

The OVMO XPS structure of the PuO$_2$Cl$_4^{2-}$ cluster has its typical features and can be subdivided into three components (1-3) at 2.9, 5.1and 7.5 eV BE, respectively (fig. 6, tab. 3). The peak at 2.9 eV BE is mostly due to the quasi-atomic Pu 5f electrons of the $20\gamma_7^-$ OVMO, which participate weakly in the chemical binding. It agrees with the calculation results (tabs. 2, 3). The fact that the calculated XPS OVMO (63.0 %) intensity is comparable with the corresponding experimental intensity (64.7 %) can be explained by the fact that the Pu 5f electrons do not lose their f-nature participating in the chemical bond. It results in the widened XPS band in the OVMO BE range of Cs$_2$PuO$_2$Cl$_4$, which agrees qualitatively with the calculation data (fig. 6, tabs. 2, 3).

Valence XPS structure of Cs$_2$PuO$_2$Cl$_4$

The IVMO range exhibits explicit peaks and can be subdivided into the seven components (4-10; fig. 6). Despite the formalism of such a division, it allows qualitative and quantitative comparison of the XPS parameters with the relativistic calculation results for the PuO$_2$Cl$_4^{2-}$ (D$_{4h}$) cluster.

Results of these calculations are given in tab. 2. Since photo-emission results are given for an excited state of an atom with a hole on a certain shell, the calculations must be done for transition states for a stricter comparison of the theoretical and experimental BE [43]. However, the valence electrons BE calculated for transition states are known to differ from the corresponding values for the ground state by a con-

stant shift toward the higher energies. Therefore, the present paper gives the calculated BE (tab. 2) shifted by 3.33 eV (tab. 3). Taking into account the MO compositions (tab. 2) and the photo-ionization cross-sections [37, 38], the theoretical intensities of several XPS ranges were determined (tab. 3). Comparing the experimental XPS to the theoretical data, one should keep in mind that the Cs$_2$PuO$_2$Cl$_4$ XPS reflects the band structure and consists of bands widened due to the solid-state effects. Despite this approximation, a satisfactory qualitative agreement between the theoretical and the experimental data was obtained (fig. 6).

Indeed, the corresponding theoretical and experimental FWHM and the relative intensities of the inner and outer valence bands are comparable (tab. 3, fig. 6). A satisfactory agreement between the experimental and calculated BE of some MO was also reached (tab. 3). For the more accurate determination of the position of the $21\gamma_6^-$ OVMO (characterizing Pu-O bond) relative to the quasi-atomic $15\gamma_7^+$, $20\gamma_6^-$, $20\gamma_6^+$ IVMO of chlorine, the calculations of PuO$_2$Cl$_4^{2-}$ electronic structure at three interatomic distances: (a) R_{Pu-O} = 0.171 nm and R_{Pu-Cl} = 0.262 nm, (b) R_{Pu-O} = 0.174 nm and R_{Pu-Cl} = 0.264 nm, (c) R_{Pu-O} = 0.176 nm and R_{Pu-Cl} = 0.266 nm were done. Going on from (a) to (b) and (c), as it was expected, the outer and the inner valence bands get narrower by 0.32 eV and 0.73 eV, respectively. The BE difference between the $15\gamma_7^-$ (5) and the $21\gamma_6^-$ (4) IVMO decreases by 0.21 eV, and the mean BE of the quasi-atomic chlorine-related IVMO ($15\gamma_7^+$, $20\gamma_6^-$, $20\gamma_6^+$) decreases by 0.15 eV. The changes in the interatomic distances do not result in any significant changes of the XPS structure and position of the $21\gamma_6^-$ IVMO relative the quasi-atomic IVMO of chlorine. These data promote the RDV method and underlie the quantitative MO scheme for understanding the nature of interatomic bonding in Cs$_2$PuO$_2$Cl$_4$.

Thus, the outer valence band intensity is formed mostly from the outer valence Pu 5f,6d,7s,7p and O 2p,Cl 3p AO, and to a lesser extent from the inner valence Pu 6p and O 2s,Cl 3s AO. The Pu 5f electrons contribute significantly to the OVMO intensity (tabs. 2 and 3). Because the Pu 5f photo-emission cross-section is high (tab. 2), the Pu 5f electrons contribute significantly to the OVMO XPS intensity if they do not lose the f-nature. Thus, the Pu 5f electrons can be promoted to *e. g.*, the Pu 6d level first, and then to participate in the chemical bond formation losing the f-nature. The calculation shows that the Pu 5f electrons participate directly in the formation of the interatomic bond (tab. 2). The calculated OVMO/IVMO intensity ratio for the PuO$_2$Cl$_4^{2-}$ XPS was found to be 1.70, which differs from the experimental value 1.82 (tab. 3) due to the error in the XPS difference spectrum.This intensity ratio is an important quantitative characteristic of the PuO$_2$Cl$_4^{2-}$ electronic structure. These results yield a conclusion that the Pu 5f electrons can participate directly in the chemical bond formation of

Yu. A. Teterin, *et al.*: Electronic Structure and Chemical Bond Nature in ...
Nuclear Technology & Radiation Protection: Year 2015, Vol. 30, No. 2, pp. 99-112

107

Table 3. Valence XPS parameters for Cs$_2$PuO$_2$Cl$_4$ and for the PuO$_2$Cl$_4^{2-}$ cluster (RDV), and orbital forces[a] f_O and f_{Cl}, Pu 6p and Pu 5f DOS ρ_i(e⁻)

MO		$-E^{[b]}$ [eV]	f_O 10⁻⁸ N	f_{Cl} 10⁻⁸ N	XPS Energy$^{[c]}$ [eV] Exper.	XPS Intensity [%] Theory	XPS Intensity [%] Exper.	Pu 6p,5f DOS ρ_i e⁻ (electrons) 5f$_{5/2}$	5f$_{7/2}$	6p$_{1/2}$	6p$_{3/2}$
OVMO	20γ_7^{-} [d]	3.33	−0.15	−0.02	2.9 (2.1)	13.6	14.0	1.46	0.30		
	25γ_6^{+}	4.13	−0.14	0.07		1.7					
	26γ_6^{-}	4.36	−0.14	0.06		2.1		0.04	0.02		0.04
	19γ_7^{+}	4.38	−0.10	0.08		1.6					
	24γ_6^{+}	4.39	−0.10	0.08		1.6					
	19γ_7^{-}	4.60	−0.14	0.09	5.1 (2.1)	2.8	25.8	0.10	0.06		0.02
	25γ_6^{-}	4.71	−0.14	0.11		3.1			0.22		
	18γ_7^{-}	4.72	−0.14	0.09		3.3		0.10	0.14		0.02
	17γ_7^{-}	4.90	−0.16	0.12		6.4		0.66	0.02		0.02
	24γ_6^{-}	5.06	−0.14	0.08		3.1		0.08	0.12		0.02
	18γ_7^{+}	5.24	−0.13	0.15		1.8					
	17γ_7^{+}	5.58	−0.13	0.13		1.9					
	23γ_6^{+}	5.73	−0.15	0.11		1.6					
	23γ_6^{-}	6.51	0.22	0.02	7.3 (2.4)	7.1	24.7	0.22	0.66	0.02	0.14
	22γ_6^{+}	7.43	0.39	0.01		0.6					
	16γ_7^{-}	7.48	0.57	0.01		4.6		0.22	0.36		0.04
	16γ_7^{+}	7.68	0.62	0.02		0.6					
	21γ_6^{+}	7.78	0.61	−0.02		0.7					
	22γ_6^{-}	7.78	0.61	−0.01		4.8		0.52	0.08	0.02	
	$\Sigma f_1^{[e]}$		1.26	1.22		63.0	64.7	3.40	2,03	0.04	0.30
			(59.4 %)	(73.1 %)							
IVMO	21γ_6^{-}	15.30	−0.40	−0.01	~15.3	3.9		0.02	0.02		0.64
	15γ_7^{-}	16.10	−0.12	0.30	16.1(2.0)	4.5	16.5				0.18
	15γ_7^{+}	16.69	−0.14	0.13		4.5					
	20γ_6^{-}	16.70	−0.20	0.11		4.5		0.02	0.02	0.02	0.06
	20γ_6^{+}	16.80	−0.14	0.13		4.5					
	14γ_7^{-}	20.52	−0.03	0.10	21.0(3.1)	4.6	7.2				1.72
	19γ_6^{+}	22.17	0.55	−0.01	25.3(3.1)	3.3	6.4				
	19γ_6^{-}	25.22	0.60	0.01	27.9(2.5)	4.1	3.0	0.02	0.02	0.32	0.90
	18γ_6^{-}	32.04	0.67	−0.01	32.0 (3.2)	3.1	2.4			1.58	0.06
	$\Sigma\rho_i^{[f]}$					37.0	35.5	0.06	0.06	1.92	3.56
	18γ_6^{+}	50.13	0.07	−0.02	51.7 (7)	~4.0					
	$\Sigma f_2^{[g]}$		0.486	0.45							
			(41.6 %)	(26.9 %)							
	$\Sigma f^{[h]}$		2.12	1.67							

[a] Orbital force per one ligand: f_O for Pu-O bond and f_{Cl} for Pu-Cl bond. Positive forces mean attraction, negative – repulsion; [b] Calculated energies (tab. 2) shifted by 3.33 eV toward the negative values (downward) so that the 15γ_7^{-} MO energy is 16.1 eV; [c] FWHM in eV given in parentheses; [d] HOMO (highest occupied MO) (2 electrons), occupation number for all the orbitals is 2; [e] the sum of the OVMO orbital forces peak intensities and the Pu 6p, 5f DOS; [f] the sum of peak intensities and the Pu 6p, 5f DOS, [g] the sum of the IVMO orbital forces; and [h] the sum of the OVMO and the IVMO orbital forces

PuO$_2$Cl$_4^{2-}$ partially losing the f-nature. These electronic states are distributed within the outer valence band (tab. 2); the Pu 6d electronic states are located mostly at the bottom of the outer valence band. The Pu 6p$_{3/2}$ AO take a significant part in the OVMO formation. This agrees with the theoretical and the experimental data for γ-UO$_3$ [16, 27] and UF$_2$O$_2$ [10].

In the IVMO XPS BE range a satisfactory agreement was reached *e. g.*, for the 21γ_6^{-} (4) and 18γ_6^{-} (10) MO responsible for the width E of this XPS band. The calculated E_{Theor} = 16.74 eV agrees with the ex-

perimental E_{exp} =16.7 eV (tab. 3). It has to be noted that the theoretical (1.70) and experimental (1.82) OVMO/IVMO intensity ratios are comparable. It confirms correctness of the approximations used in the calculation (tab. 3). The calculated and the experimental relative intensities of some individual IVMO peaks, except for the 21γ_6^{-} (4), 14γ_7^{-} (7), 19γ_6^{+} (8) ones, are in a qualitative agreement.

Taking into account the experimental BE differences between the outer MO and the core levels in the PuO$_2$Cl$_4^{2-}$ cluster and metallic Pu [35], as well as the

108

Yu. A. Teterin, *et al*.: Electronic Structure and Chemical Bond Nature in ...
Nuclear Technology & Radiation Protection: Year 2015, Vol. 30, No. 2, pp. 99-112

relativistic MO LCAO calculation data for the $PuO_2Cl_4^{2-}$ (D_{4h}) cluster, a quantitative MO scheme for this cluster (fig. 7) was built. This scheme allows one to understand the real XPS structure and the chemical bond nature in the $PuO_2Cl_4^{2-}$ cluster. In this approximation, one can pick out the antibonding $21\gamma_6^-$ (4) and $15\gamma_7^-$ (5) and the corresponding bonding $19\gamma_6^-$ (9) and $14\gamma_7^-$ (7) IVMO, as well as the quasi-atomic $15\gamma_7^+$, $20\gamma_6^-$, $20\gamma_6^+$ (6), and $19\gamma_6^+$ (8) ones attributed mostly to the Cl 3s and O 2s electrons. The experimental data show that the Cl 3s-related quasi-atomic IVMO BE have to be close by magnitude.

Indeed, the Cl 3s XPS peak of CsCl [E_b(Cl 3s) = 15.0 eV] is 1.2 eV wide. In $Cs_2PuO_2Cl_4$ XPS this peak is observed at E_b(Cl 3s) = 16.1 eV and is 1.8 eV wide (tab. 1). The BE shift and widening is associated with the Cl 3s AO participation in the IVMO formation (fig. 5). The Cs 5p XPS was observed as a spin-orbit split doublet in the band-gap between the OVMO and IVMO at E_b(Cs $5p_{3/2}$) = 10.4 eV and E_{sl}(Cs 5p) = 1.7 eV fig. 5(a). The Cs 5s peak in the $Cs_2PuO_2Cl_4$ XPS was observed single at E_b(Cs 5s) = 23.7 eV and Γ(Cs 5s) = 1.3 eV. It was superimposed with the O 2s peak attributed to the plutonyl group PuO_2^{2+}. It has to be noted that cesium peaks were observed intense in the whole BE range 10 eV-1250 eV. The Cs XPS of CsCl exhibits an extra structure at the higher BE side from the basic peaks E_{sat1} = 9.4 eV and E_{sat2} = 23.4 eV. It can be attributed to the electron energy loss processes during photo-emission. Such a structure was observed in the core chlorine XPS of CsCl at E_{sat3} = 19.3 eV see *e. g.* fig. 5(b). This structure complicates interpretation of the valence $Cs_2PuO_2Cl_4$ XPS. The O 1s peak was observed symmetric and 1.8 eV wide (fig. 1), while the BE of the quasi-atomic $19\gamma_6^+$ (8) IVMO should be about 23.8 eV since E_O = 508 eV and the O 1s BE in $Cs_2PuO_2Cl_4$ XPS is E_b(O 1s) = 531.8 eV (tab. 1). These data partially agrees with the theoretical results. Taking into account that the experimental E_{Pu} = 404.9 eV [35] is comparable with the calculated value 403.8 eV [36], and the difference E_1 = 413.4 eV, one can find that $\Delta_1 = E_1 - E_{Pu}$ is 8.5 eV (fig. 7). Since the BE difference between the $21\gamma_6^-$ (4) and $18\gamma_6^-$ (10) IVMO is 16.7 eV, and the Pu 6p spin-orbit splitting according to the calculation data [36] is E_{sl}^t(Pu 6p) = 11.9 eV and that according to the experimental data – 12.0 eV [35], one can evaluate that the perturbation Δ_1 = 4.7 eV does not agree with the corresponding value of 8.5 eV found from the BE difference between the core and the valence MO. This difference must be attributed to the IVMO formation peculiarities and such a comparison can be not quite correct. However, these data show that the $21\gamma_6^-$ (4) IVMO has a significant antibonding nature. The IVMO FWHM cannot yield a conclusion on the IVMO nature (bonding or antibonding), however, one can suggest that the admixture of 9 % of O 2p and 2 % of Pu 5f AO in the $21\gamma_6^-$ (4) IVMO leads these orbitals

to loosing of their antibonding nature (tab. 2, fig. 7, see also [6]). Thus, the quantitative MO scheme for $PuO_2Cl_4^{2-}$ built on the basis of the experimental and the theoretical data allows one both to understand the nature of chemical bond formation in $Cs_2PuO_2Cl_4$ and to interpret the structures of other X-ray spectra as it was shown for γ-UO_3 [16, 26, 27] and UO_2F_2 [10].

Chemical bond in the $PuO_2Cl_4^{2-}$ cluster

As it was noted, the calculation data show that the MO system of the $PuO_2Cl_4^{2-}$ cluster can be subdivided into several groups (tab. 2, fig. 7). One group associated with the plutonyl ion PuO_2^{2+} includes the $18\gamma_6^+$, $18\gamma_6^-$ (10), $19\gamma_6^-$ (9), $19\gamma_6^+$ (8), and $21\gamma_6$ (4) IVMO characterizing the Pu-O bond in the axial direction. Another group from the $14\gamma_7^-$ (7) to the $15\gamma_7^-$ (5) IVMO consists of the Cl 3s and Pu 6p AO. Moreover, another one – from the $22\gamma_6^-$ to the $20\gamma_7^-$ OVMO represents the valence band. In the lower part of this band there are the 2p-type bonding MO with the admixtures of Pu valence states, the middle and the upper parts – consist of the Cl 3p MO with admixtures of metal MO (tab. 2).

In the Koopmans' theorem approximation, the orbital forces f_i (10^{-8} N) approximately are equal to the derivatives of the MO energies E_i' (10^{-8} N) upon the interatomic distances [6]. This work presents the dependence of the MO energies for the $PuO_2Cl_4^{2-}$ cluster on the interatomic distance in the axial direction R_{Pu-O} (Z-axis) and in the equatorial plane R_{Pu-Cl}. To evaluate the orbital forces beside the calculation for the equilibrium atomic positions (R_{Pu-O} = 0.1752 nm, R_{Pu-Cl} = = 0.2665 Å*), two more calculations were also done. One for R_{Pu-O} = 0.1772 Å and the invariable positions of chlorine ions, and another one – with equal positions of oxygen ions but with increased Pu-Cl distance to the four chlorine ions R_{Pu-Cl} = 0.2685 Å. It yielded the orbital forces f_i (derivatives E_i' of the OVMO and IVMO energies E_i upon the interatomic distances R_{Pu-O} and RP_{u-Cl}) (tab. 3).

As it follows from tab. 3 and the MO scheme (fig.7), the $18\gamma_6^+$, $18\gamma_6^-$ (10), $19\gamma_6^-$ (9), $19\gamma_6^+$ (8) IVMO from this group bring a significant bonding contribution (1.89 10^{-8} N) to the Pu-O binding and a slight antibonding contribution (–0.03 10^{-8} N) to the Pu-Cl interaction. On the other hand, the IVMO of the other group from the $14\gamma_7^-$ (7) to the $15\gamma_7^-$ (5) containing the Cl 3s states bring a significant bonding contribution (0.50 10^{-8} N) to the Pu-Cl interaction and an antibonding contribution (–1.03 10^{-8} N) to the Pu-O binding. As it was expected, the bonding OVMO surrounds the valence band bottom ($22\gamma_6^-$ -$23\gamma_6^-$) contributes significantly (3.02 10^{-8} N) to the Pu-O binding even despite the antibonding nature (–1.76 10^{-8} N) of

---

*1 Å = 10^{-10} m
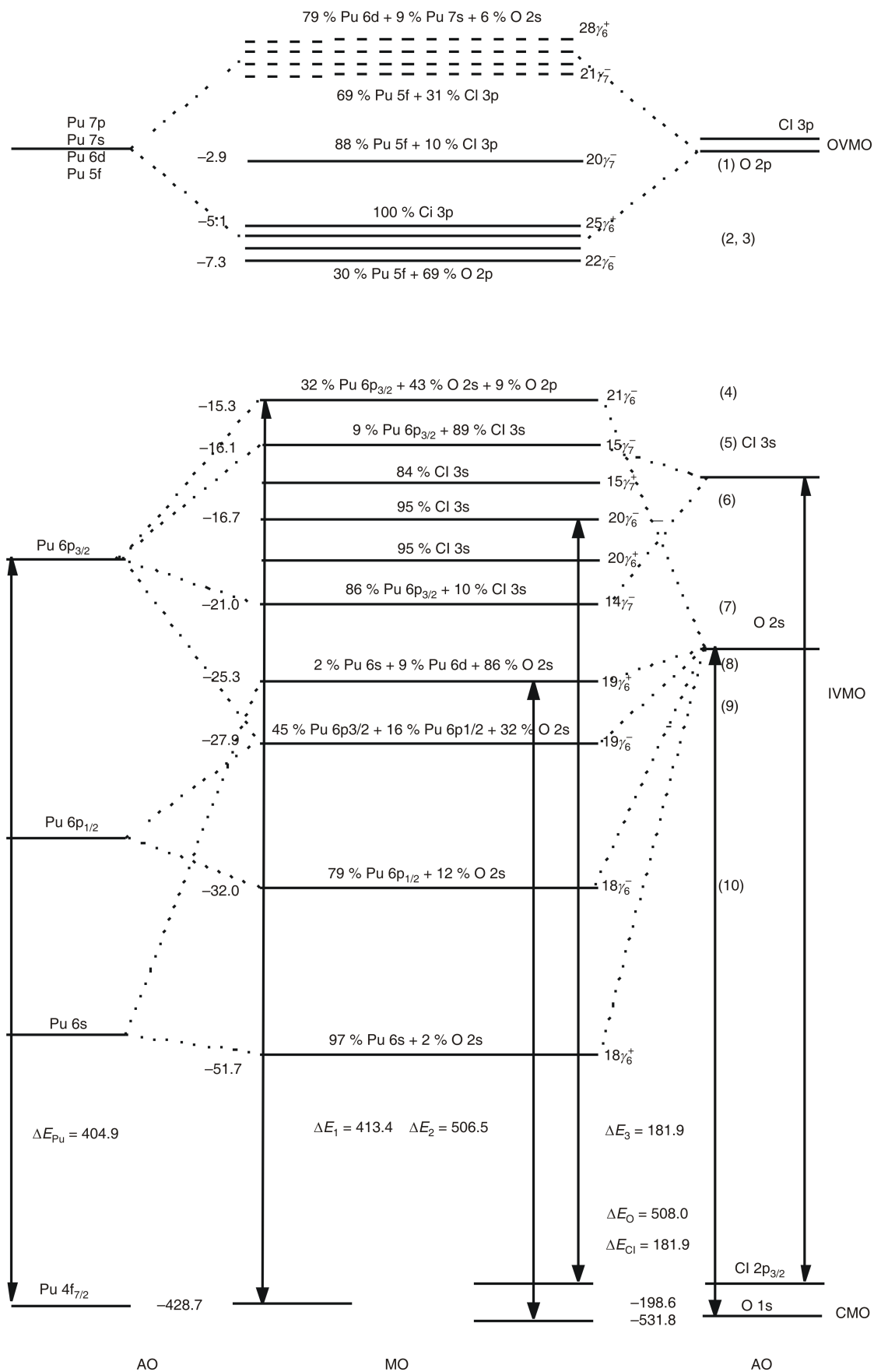
Figure 7. MO scheme for the PuO$_2$Cl$_4^{-2}$ [D$_{4h}$] cluster built taking into account theoretical and experimental data. Chemical shifts are not indicated. Arrows show some measurable levels BE differences. Experimental BE [eV] are given to the left. The energy scale is omited

110

Yu. A. Teterin, *et al*.: Electronic Structure and Chemical Bond Nature in ...
Nuclear Technology & Radiation Protection: Year 2015, Vol. 30, No. 2, pp. 99-112

the other OVMO of this group. The total OVMO contribution to the Pu-O bond is 1.26 10^{-8} N. The total OVMO contribution to the Pu-Cl binding per one bond is 1.22 10^{-8} N, which is comparable to that for the Pu-O bond. On the basis of these data the relative IVMO contribution to the Pu-O binding per one bond in the PuO$_2$Cl$_4^{2-}$ cluster was evaluated as 40.6 %, and that of the OVMO contribution – 59.4 %.The relative IVMO contribution to the Pu-Cl binding is 26.9 %, that of the OVMO – 73.1 % (tab. 3).

On the basis of the structures of irreducible representations of the D$_{4h}$ group, the Pu 6d and the Pu 5f AO participations in the chemical bond were compared [33]. Table 3 shows that among the six bonding MO in the lower part of the valence band there are three orbitals of each type. The share of the 6d AO in the $21\gamma_6^+$, $16\gamma_7^+$, and $22\gamma_6^+$ MO are 0.18, 0.17, and 0.3, respectively, while the share of the 5f AO in the $22\gamma_6^-$, $16\gamma_7^-$, and $23\gamma_6^-$ MO are 0.30, 0.29, and 0.45, respectively (tab. 2). Despite the fact that the share of the 5f AO is greater than that of the 6d AO, their contributions are comparable, and the last $23\gamma_6^-$ orbital shows the least orbital force (0.22 10^{-8} N) among the six considered bonding MO. Among the Pu-Cl bond-related OVMO, the upper MO starting with the $23\gamma_6^+$ show the highest orbital forces.The bonding role of the 6d states in the Pu-Cl binding is also slightly higher than that of the 5f states. These results agree with the values of the overlapping populations for the corresponding orbitals found in the present work. These results also agree with the data on the covalent contribution of the uranyl group UO$_2^{2+}$ with R_{U-O} = 0.173 Å to the IVMO [6]. For uranyl group the method of the full energy separation and X -DV determination of the resonance energy E^R(eV) showed that the IVMO electrons contribution to the covalent component of the chemical bond is 37 % of the total contribution of all the MO [6]. Despite the approximation used for the evaluation of these data was not perfect, one can conclude that the theoretical and experimental studies of chemical bond cannot neglect the IVMO formation effect in actinide compounds.

CONCLUSIONS

With the core electron XPS structure, BE differences between the core and the valence electronic levels and the relativistic calculation results of the electronic structure of the PuO$_2$Cl$_4^{2-}$ (D$_{4h}$) cluster in mind, a quantitative interpretation of the valence XPS structure in the BE range 0-~35 eV for Cs$_2$PuO$_2$Cl$_4$, was done. The correlation of the XPS structure parameters with the mechanisms of its formation was established. The Pu 5f (3.79 Pu 5f e$^-$) electrons delocalized within the outer valence band were theoretically shown and experimentally confirmed to participate directly in the chemical bond formation in Cs$_2$PuO$_2$Cl$_4$ partially losing their *f*-nature. The other part of the Pu 5f electrons (1.76 Pu 5f e$^-$) was shown to be localized mostly at 2.9 eV BE. The Pu 6p electrons, in addition to the effective (experimentally measurable) participation in the IVMO formation, were found to participate noticeably (0.34 Pu 6p e$^-$) in the filled OVMO formation. The greatest part in the IVMO formation in Cs$_2$PuO$_2$Cl$_4$ was established to be taken by the Pu 6p$_{1/2,3/2}$ and the O 2s AO, and to a lesser extent – by the Pu 6p$_{3/2}$ and Cl 3s AO of the neighboring plutonium oxygen and chlorine ions. The MO sequent order in the BE range of 0-~35 eV for the PuO$_2$Cl$_4^{2-}$ cluster was defined and the corresponding MO composition was obtained. It allowed a fundamental quantitative MO scheme, which is important for understanding the nature of interatomic bonding in PuO$_2$Cl$_4^{2-}$ and for the interpretation of other X-ray spectra. The OVMO and IVMO contributions to the chemical bond were evaluated for the PuO$_2$Cl$_4^{2-}$ cluster. The relative OVMO contribution to the chemical binding was shown to be 66 %, and that of the IVMO – 34 %. Despite the approximation used for the evaluation of the IVMO, OVMO contributions was not perfect, one can conclude that the theoretical and experimental studies of chemical bond cannot neglect the IVMO formation effect in actinide compounds.

AUTHORS CONTRIBUTIONS

The idea for the study was put forward by Yu. A. Teterin, the measurements were carried out by K. I. Maslakov, the theoretical calculations were carried out by M. V. Ryzhkov, the compounds were produced by D. N. Suglobov, the samples were prepared, the experimental data were processed and interpreted by A. Yu. Teterin, K. E. Ivanov, S. N. Kalmykov and V. G. Petrov.

REFERENCES

[1] Verbist, J., *et al*., X-Ray Photoelectron Spectra of Uranium and Uranium Oxides, Correlation with the Half-Life of ^{235}Um, *J. Electr. Spectr. Relat. Phenom., 5* (1974), 1, pp. 193-205

[2] Veal, B. W., *et al.*, X-Ray Photoelectron Spectroscopy Study of Hexavalent Uranium Compounds, *Phys. Rev. B, 12* (1975), 12, pp. 5651-5663

[3] Teterin, Yu. A., *et al*., A study of Synthetic and Natural Uranium Oxides by X-Ray Photoelectron Spectroscopy, *Physics and Chemistry of Minerals, 7* (1981), 4, pp. 151-158

[4] Teterin, Y. A., *et al.*, Low-Energy X-Ray Photoelectron Spectral Structure of Oxides UO$_2$ and γ-UO$_3$, *Doklady Akademii Nauk SSSR (Reports of the Academy of Sciences of USSR), 256* (1981), 2, p. 381

[5] Thibaut, E., *et al*., Electronic Structure of Uranium Halides and Oxyhalides in the Solid State, An X-Ray Photoelectron Spectroscopy Study of Bonding Iconicity, *J. Am. Chem. Soc., 104* (1982), 20, pp. 5266-5273

[6] Teterin, Yu. A., Gagarin, S. G., Inner Valence Molecular Orbitals and the Structure of X-Ray Photoelectron Spectra, *Russian Chemical Reviews, 65* (1996), 10, pp. 825-847

[7] Teterin, Yu. A., Teterin, A. Yu., Structure of X-Ray Photoelectron Spectra of Light Actinide Compounds, *Russian Chemical Reviews, 73* (2004), 6, pp. 541-580

[8] Teterin, Y. A., *et al.*, XPS Structure of $Cs_3NpO_2Cl_4$ and $Cs_2NpO_2Cl_4$ Single Crystals, *Doklady Akademii Nauk SSSR (Reports of the Academy of Sciences of USSR), 276* (1984), 1, pp. 154-159

[9] Teterin, Y. A., *et al.*, Correlation of the XPS Structure of Plutonium and Uranium in $Cs_2AnO_2Cl_4$ (An = Pu, U) Crystals with Oxidation States, Structure and Chemical Bond Nature, *Doklady Akademii Nauk SSSR (Reports of the Academy of Sciences of USSR), 277* (1984), 1, pp. 131-136

[10] Utkin, I. O., *et al.*, Study of the Electronic Structure of Uranyl Fluoride UO_2F_2, *Radiochemistry, 47* (2005), 4, pp. 334-344

[11] Teterin, Yu. A., Teterin, A. Yu., Structure of X-Ray Photoelectron Spectra of Lanthanide Compounds, *Russian Chemical Reviews, 71* (2002), 5, pp. 347-381

[12] Boring, M., Wood, J. H., Miscowitz, J. M., Self-Consistent Field Calculation of the Electronic Structure of the Uranyl Ion (UO_2^{++}), *J. Chem. Phys., 63* (1975), 2, pp. 638-642

[13] Ellis, D. E., Rosen, A., Walch, P. F., Applications of the Dirac-Slater Model to Molecules, *Intern. J. Quant. Chemist. Symp., 9* (1975), Suppl. S9, pp. 351-358

[14] Walch, P. F., Ellis, D. E., Effects of Secondary Ligands on the Electronic Structure of Uranyls, *J. Chem. Phys., 65* (1976), 6, pp. 2387-2392

[15] Hirata, M., *et al.*, Valence Electronic Structure of Uranyl Nitrate $UO_2(NO_3)_2$ $2H_2O$, *J. Electr. Spectr. Relat. Phenom., 83* (1997), 1, pp. 59-64

[16] Teterin, Yu. A., *et al.*, The Structure of the Valence Electronic Orbitals in Uranium Trioxide γ-UO_3, *J. Nucl. Sci. Technol., 3* (2002), Suppl. 3, pp. 74-77

[17] Denning, R. G., Electronic Structure and Bonding in Actinyl Ions, *Structure and Bonding, 79* (1992), pp. 215-276

[18] Denning, R. G., Electronic Structure and Bonding in Actinyl Ions and Their Analogs, *J. Chem. Phys. A, 111* (2007), 20, pp. 4125-4143

[19] Atuchin, V. V., Zhang, Z., Chemical Bonding Between Uranium and Oxygen in U^{6+}-Containing Compounds, *J. Nucl. Mater., 420* (2012), 1-3, pp. 222-225

[20] Teterin, Yu. A., *et al.*, The Role of the low-Energy Filled Shells Electrons of Neighboring Atoms in the Chemical Bond of Uranium Compounds (in Russian), *Doklady Akademii Nauk SSSR (Reports of the Academy of Sciences of USSR), 284* (1985), 4, p. 915

[21] de Jong, W. A., Visscher, L., Nieupoort, W. C., On the Bonding and the Electric Field Gradient of the Uranyl Ion, *J. Molecular Structure (Theochem), 458* (1999), 1-2, pp. 41-52

[22] Teterin, Y. A., *et al.*, Electronic Structure and Chemical Bonding in PuO_2, *Phys. Rev. B, 87* (2013), 24, 245108

[23] Bjorkman, T., Eriksson, O., Coupling between the 4f Core Binding Energy and the 5f Valence Band Occupation of Elemental Pu and Pu-Based Compounds, *Phys. Rev. B, 78* (2008), 24, 245101

[24] Teterin, Y. A., *et al.*, XPS Study of the An5f Electronic States in Actinide (Th, U, Np, Pu, Am, Cm, Bk) Compounds, *J. Nucl. Sci. Technol.* (2002), Suppl. 3, pp. 140-143

[25] Ryzhkov, M. V., *et al.*, Actinile Compounds of Neptunium and Plutonium: X-Ray Photoelectron Spectra, Quantum-Chemical Calculations, *Radiochemistry, 34* (1992), pp. 69-76

[26] Teterin, Yu. A., *et al.*, Inner Valence Molecular Orbitals and Structure of X-Ray $O_{4,5}$ (Th, U) Emission Spectra in Thorium and Uranium Oxides, *Journal of Electron Spectroscopy and Related Phenomena, 96* (1998), 1-3, pp. 229-236

[27] Teterin, Y. A., *et al.*, X-Ray Spectral Determination of Density of th Valence U 6p, 5f- States in Trioxide γ-UO_3, *Radiochemistry, 44* (2002), pp. 224-232

[28] Hall, D., Rae, A. D., Waters, T. N., The Crystal Structure of Dicasium Tetrachlorodioxourannium (VI), *Acta Cryst., 20* (1966), 2, pp. 160-162

[29] Wilkerson, M. P., Scott, B. L., Dicaesium Tetrachloridodioxidoplutonat (VI), *Acta Cryst., E64, i5* (2008), sup-1 - sup-6

[30] Gouder, T., Havela, L., Examples of Quantification in XPS on 5f Materials, *Mikrochim. Acta, 138* (2002), pp. 207-215

[31] Morrall, P., *et al.*, Determination of the Clear 4f Peak Shape in XPS for Plutonium Metal, *J. Nucl. Mater., 385* (2009), 1, pp. 15-17

[32] Watkin, D. J., Denning, R. G., Prout, K., Structure of Dicaesium Tetrachlorodioxouranium (VI), *Acta Crystallogr., C47* (1991), pp. 2517-2519

[33] Teterin, Yu. A., *et al.*, Electronic Structure and Chemical Bonding in PuO_2, *Phys. Rev. B, 87* (2013), 245108

[34] Teterin, Y. A., *et al.*, The X-Ray Photoelectron Study of Actinide (Th, U, Pu, Am) Nitrates, *Nucl Technol Radiat, 18* (2003), 2, pp. 31-35

[35] Baptist, R., *et al.*, X-Ray Photoelectron Study of Plutonium Metal, *J. Phys. Ser. F, 12* (1982), pp. 2103-2114

[36] Huang, K. N., *et al.*, Neutral-Atom Electron Binding Energies from Relaxed-Orbital Relativistic Hartree-Fock-Slater Calculations 2 Z 106, *Data Nucl. Data Tables, 18* (1976), 3, pp. 243-291

[37] Band, M., Kharitonov, Y. I., Trzhaskovskaya, M. B., Photoionization Cross Sections and Photoelectron Angular Distribution for X-Ray Line Energies in the Range 0.132-4.509 keV (Targets: 100 Z 1), At. *Data Nucl. Data Tables, 23* (1979), 5, pp. 443-505

[38] Yarzhemsky, V. G., *et al.*, Photoionization Cross-Sections of Ground and Excited Valence Levels of Actinides, *Nucl Technol Radiat, 27* (2012), 2, pp. 103-106

[39] Veal, B. W., Diamond, H., Hoekstra, H. R., X-Ray Photoelectron Spectroscopy Study of Oxides of the Transuranium Elements Np, Pu, Am, Cm, Bk, and Cf, *Phys. Rev. B, 15* (1977), 6, pp. 2929-2942

[40] Yarzhemsky, V. G., Teterin, Y. A., Sosulnikov, M. I., Dynamic Dipolar Relaxation in X-Ray Photoelectron Spectra of Ba 4p Subshell in Barium Compounds, *J. Electron Spectrosc. Relat. Phenom., 59* (1992), 3, pp. 211-222

[41] Yarzhemsky, V. G., *et al.*, The Structure of the 4p X-Ray Photoelectron Spectra of Xe and Cs, Ba, La Compounds (in Russian), *J. of Surface Investigations: X-Ray, Synchrotron and Neutron Techniques, 6* (2005), pp. 3-8

[42] Amusia, M., Chernysheva, L., Yarzhemsky, V., Handbook of Theoretical Atomic Physics: Data for Photon Absorption, Electron Scattering, and Vacancies Decay. Springer, 2012

[43] Slater, J. C., Johnson, K. H., Self-Consist Field X Cluster Method for Polyatomic Molecules and Solids, *Phys. Rev. B, 5* (1972), 3, pp. 844-853

Yu. A. Teterin, *et al.*: Electronic Structure and Chemical Bond Nature in ...
Nuclear Technology & Radiation Protection: Year 2015, Vol. 30, No. 2, pp. 99-112

112

Јуриј А. ТЕТЕРИН, Константин И. МАСЛАКОВ, Михаил В. РИЖКОВ,
Антон Ј. ТЕТЕРИН, Кирил Е. ИВАНОВ, Степан Н. КАЛМИКОВ,
Владимир Г. ПЕТРОВ, Дмитриј Н. СУГЛОБОВ

ЕЛЕКТРОНСКА СТРУКТУРА И ПРИРОДА ХЕМИЈСКЕ ВЕЗЕ У Cs₂PuO₂Cl₄

Извршена је рендгенска фотоелектронска спектрална анализа једноставног кристала $Cs_2PuO_2Cl_4$ у области енергија везе од 0 до ~35 eV на основу енергија везе и структуре електронских љуски језгра (~35 eV-1250 eV), као и резултата релативистичких дискретних варијационих прорачуна за $PuO_2Cl_4{}^{2-}$ (D_{4h}). Овај кластер одражава блиску околину плутонијума у $Cs_2PuO_2Cl_4$ укључујући плутонил групу $PuO_2{}^{2+}$. Показано је да дејства више тела услед присуства цезијума и хлора доприносе спољашњој валентној спектралној структури (енергија везе од 0 до ~15 eV) много мање него унутрашњој (енергија везе од ~15 eV-~35 eV). Теоријски је прорачунато и експериментално потврђено да су унета Pu 5f електронска стања присутна у валентној зони $Cs_2PuO_2Cl_4$. То поткрепљује претпоставку о непосредном уделу Pu 5f електрона у хемијској вези. Показано је да Pu 6p атомске орбите учествују у настанку и унутрашњих и спољашњих валентних молекулских орбита (зона), док је нађено да унете електронске љуске Pu 6p, O 2s и Cl 3s имају највећи удео у настанку унутрашњих валентних молекулских орбита. Установљена је композиција молекулских орбита и секвенцијални поредак у $Cs_2PuO_2Cl_4$ у области енергије везе од 0 до ~35 eV. На основу експерименталних и теоријских података изграђена је квантитативна шема молекулских орбита за $Cs_2PuO_2Cl_4$ у области енергије везе од 0 до ~15 eV. То је битно и за разумевање природе хемијске везе у $Cs_2PuO_2Cl_4$ и за тумачење других рендгенских спектара $Cs_2PuO_2Cl_4$. Процењено је да доприноси спољашњих валентних молекулских орбита хемијском везивању $Cs_2PuO_2Cl_4$ – кластера износе 66 %, а доприноси унутрашњих 34 %.

Кључне речи: рендгенска фотоелектронска спектроскопија, плутонил група,
валентна молекулска орбита